Structure of 1-(Arylselanyl)naphthalenes − Y Dependence in 1-(*p*-$YC_6H_4Se)C_{10}H_7$

Warô Nakanishi,*[a] Satoko Hayashi,[a] and Tetsutaro Uehara[b]

Keywords: Biaryl compounds / Selenium / Through-bond interactions / Substituent effects

The structures of 1-(arylselanyl)naphthalenes [1-(*p*-YC_6H_4-Se)$C_{10}H_7$ (**1**), where Y = H (**a**), OMe (**b**), Me (**c**), Cl (**d**), Br (**e**), COOEt (**f**), and NO_2 (**g**)] were determined. The structures of **1** were well classified using types **A**, **B**, and **C**, where the Se–C_{Ar} bond in **1** is placed almost perpendicular to the naphthyl plane in type **A** and is located on the plane in type **B**. The type **C** structure is intermediate between type **A** and type **B**. The structures of **1d**–**1f** are demonstrated to be type **A** whereas that of **1b** is type **B** by X-ray crystallographic analysis. The type **B** conformer is suggested to be favorable in solutions for **1a** and **1c** based on the NMR-spectroscopic data. The structure of **1g** is assumed to be type **A**. These results show that the stable structure of **1** must be type **A** or type **B**, contrary to early observations of type **C** for 1,8-bis(alkyl- or arylchalcogeno)naphthalenes. Consequently, the structure of **1** changes dramatically depending on Y in the solid state. We propose that these structures can be explained by the electron affinities, together with the energies of LUMO and LUMO+1 of benzene, substituted benzenes, and naphthalene, which are the components of **1**. In order to clarify the reason for the dramatic change in the structure of **1** with change in Y, ab initio MO calculations were performed on **1** and related compounds. The type **A** and type **B** conformations were optimized as stable molecules. Although **1a** (type **A**) is predicted to be more stable than **1a** (type **B**) by 1.3 kJ mol^{-1}, the latter becomes more stable than the former by 8.4 kJ mol^{-1} if the solvent effects of chloroform are taken into account in the calculations, which was done by applying the IPCM method. The transition state between type **A** and type **B** in **1a** is similar to type **C**, which must prevent the monotonical change in the structure of **1**. Compound **1** would be in equilibrium between type **A** and type **B** in solutions. The results of the MO calculations on **1** suggest that type **A** is exclusive for **1g**, and probably exclusive for **1f**, and predominant for **1d** and **1e**, while type **B** is predominant for **1b**. The type **A** and type **B** would be comparable for **1a** and **1c**.

Introduction

Much attention has been paid to the chemistry brought about by the lone pairs of heteroatoms from group-16 elements.[1] The nonbonded interactions caused by the lone pairs are also of current interest.[2−6] Lone pair−lone pair interactions have been demonstrated to play an important role in the nonbonded spin−spin couplings between the heteroatoms.[3,4c,4d,4f,7−9] We have investigated the nonbonded interactions arising from direct orbital overlaps containing lone pair orbitals of group-16 elements.[4] It is important to set up the system to show detectable interactions, since the interactions are usually very weak. A nonbonded G···M distance of nearly the sum of van der Waals radii minus 1 Å is desirable for the obvious orbital overlap. The naphthalene 1,8-positions should provide a good system to investigate such nonbonded interactions, since the nonbonded distances between G and M in 8-G-1-$MC_{10}H_6$ are very close to the sum of van der Waals radii minus 1.0 Å.[10] Characteristic structures have been reported for 8-G-1-(*p*-$YC_6H_4Se)C_{10}H_6$, together with the factors used to determine the structures, based on the nonbonded G···Se interactions.

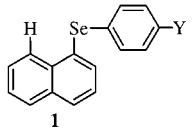

1

	a	b	c	d	e	f	g
Y =	H	OMe	Me	Cl	Br	CO_2Et	NO_2

As further work is done on the nonbonded G···Se interactions in 8-G-1-(*p*-$YC_6H_4Se)C_{10}H_6$, it becomes imperative to establish the basic structure with no influence of the nonbonded interactions. The structures were determined for 1-(*p*-$YC_6H_4Se)C_{10}H_7$ [**1**: Y = H (**a**), OMe (**b**), Me (**c**), Cl (**d**), Br (**e**), COOEt (**f**), and NO_2 (**g**)]. The structures of **1b** and **1d**−**1f** were investigated by X-ray crystallographic analysis, and those of **1a** and **1c** were studied based on NMR-spectroscopic data. Ab initio MO calculations were also performed on **1a** and related compounds to clarify the structural feature of **1**.

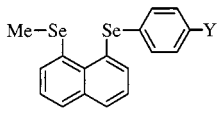

2

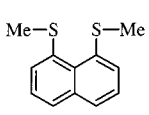

3

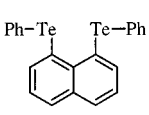

4

[a] Department of Material Science and Chemistry, Faculty of Systems Engineering, Wakayama University,
930 Sakaedani, Wakayama 640-8510, Japan
Fax: (internat.) + 81-73/457-8253
E-mail: nakanisi@sys.wakayama-u.ac.jp
[b] Department of Computer and Communication Sciences, Faculty of Systems Engineering, Wakayama University
930 Sakaedani, Wakayama 640-8510, Japan

  1434−193X/01/1020−3933 $ 17.50+.50/0

The structures of 8-(MeSe)-1-(*p*-YC_6H_4Se)$C_{10}H_6$ [**2a** (Y = H)],[4e] 1,8-bis(methylsulfanyl)naphthalene (**3**),[2b] and 1,8-bis(phenyltelluro)naphthalene (**4**)[3a] are reported. They have a common character among a number of structures studied for 1,8-disubstituted naphthalenes by X-ray crystallographic analysis.[2b,3a,4c,4d,4f,10,11] The chalcogen−carbon bonds decline 30−50° from the naphthyl plane. The structure is called type **C** as shown in Scheme 1.[4e] The type **C** structure has been demonstrated to avoid the severe exchange repulsion between lone pairs in **2a**.[4e] One may imagine from the observations that the type **C** structure is the basic one for compound **1**. The structure of pseudo C_2 symmetry reported for ditolyl selenide (**5**)[12] might also support the type **C** structure for **1**. Nevertheless, the structure around the Se atom in **1** could be very different from those of **2a**, **3**, and **4**.

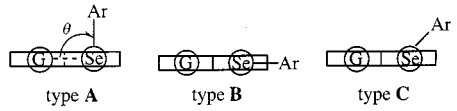

Scheme 1. Types of structures in 8-G-1-(*p*-YC_6H_4Se)$C_{10}H_6$

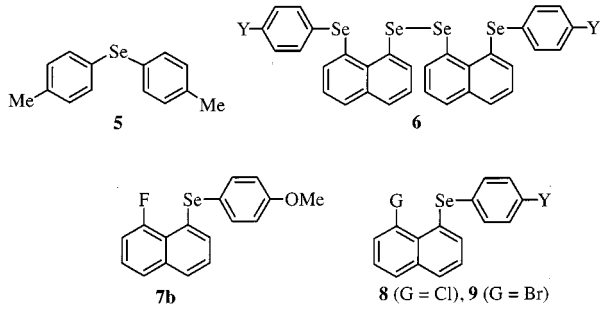

Recently, type **A** and type **B** structures (type **A**−type **B** pairing) have been reported around the PhSe and Se−Se moieties, respectively, in 1-[8-(*p*-YC_6H_4Se)$C_{10}H_6$]Se-Se[$C_{10}H_6$(SeC_6H_4Y-*p*)-8′]-1′ [**6a** (Y = H)].[4e] The type **A**−type **B** pairing is also found in **2b** (Y = OMe) and **2d** (Y = Cl),[4g] although **2b** contains some type **C** character observed in **2a**. The type **A**−type **B** pairing must be stabilized by the electron donor−acceptor interaction through the nonbonded Se···Se−X three centers − four electrons interactions (3c−4e), where X = Se for **6a** and X = C for **2b** and **2d**. The type **B** structure is also confirmed around the Se atom in 8-fluoro-1-(*p*-anisylselanyl)naphthalene (**7b**),[4d] together with the 8-chloro- and 8-bromo derivatives of **1** (**8** and **9**, respectively).[13,14]

A plot of ^{77}Se NMR chemical shifts [δ(Se)] of 8-G′-1-(*p*-YC_6H_4Se)$C_{10}H_6$ versus those of 8-G-1-(*p*-YC_6H_4Se)$C_{10}H_6$ should give a very good correlation[14] if the structures around the Se atoms of the compounds are substantially the same. However, the plots of δ(Se) of *p*-YC_6H_4Se groups in **2** and **6** versus those of **1** did not give good correlations.[4c,15a,15b] The δ(Se) values of *p*-YC_6H_4SePh (**10**) gave a better correlation instead, when δ(Se) of **10** were used as the abscissa.[15c] These observations must be a reflection of the characteristic structure of **1**, relative to those of **2** and **6**.

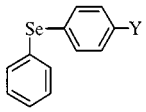

10

The results led us to a working hypothesis that stable conformers of **1** must be very different from those in **10**. The latter are commonly described by the fourfold torsional potential with nonplanar and nonperpendicular stable structures.[16] The type **A** and type **B** structures must be the basic ones for **1**, in spite of earlier observations of type **C** in **2a**, **3**, and **4**.

Results and Discussion

Structures of 1-(*p*-YC_6H_4Se)$C_{10}H_7$ (1)

Single crystals of **1b** and **1d**−**1f** were obtained by slow concentration of hexane solutions, and one of the suitable crystals from each compound was subjected to X-ray crystallographic analysis. Their crystallographic data are summarized in Table 1. Only one type of structure corresponds to each of them in the crystals. The structures of **1b** and **1d**−**1f** are shown in Figures 1, 2, 3, and 4, respectively. The selected interatomic distances, angles, and torsional angles of **1b** and **1d**−**1f** are collected in Table 2. The X-ray crystallographic analysis could not be carried out for **1a** and **1c**, because of their oily property at ambient temperatures (around 20 °C). The single crystal of **1g** was too thin to determine its structure by the X-ray crystallographic analysis.

As shown in Figure 1, the planarity of the naphthyl (Nap) and anisyl (An) planes in **1b** is very good: It is little perturbed by substitution with the Se atom. The anisyl plane is perpendicular to the naphthyl plane, with the torsional angle C(1)−Se−C(11)−C(16) being −77.6(3)°. The Se−C_{An} bond lies on the naphthyl plane, and the torsional angles of Se−C(1)−C(10)−C(9) and C(11)−Se−C(1)−C(10) are 3.9(4)° and 178.9(2)°, respectively. The C_{Nap}−Se−C_{An} angle [C(1)−Se−C(11)] is 102.1(1)°. The structure of **1b** belongs to type **B**; it is described as **1b** (type **B**).

On the other hand, the structures around the selenium atoms in **1d**−**1f** are very different from that of **1b**. The structures of these compounds are explained using **1d**, which is shown in Figure 2. The planarity of the naphthyl and *p*-chlorophenyl planes (*p*-ClC_6H_4: Ar) is also good. The Se−C_{Ar} bond is perpendicular to the naphthyl plane with torsional angles of Se−C(1)−C(10)−C(9) and C(11)−Se−C(1)−C(10) being −2.0(4)° and 79.3(3)°, respectively. The *p*-chlorophenyl plane is perpendicular to the naphthyl plane [the torsional angle C(1)−Se−C(11)−C(16) is −5.9(3)°]. The C_{Nap}−Se−C_{Ar} angle [C(1)−Se−C(11)] is 99.3(1)°. The structure of **1d**, together with those of **1e** and **1f**, belongs to type **A**.

Table 3 collects bond lengths, angles, and the torsional angles around the selenium atoms in **1b** and **1d**−**1f**, to-

Table 1. Selected crystal data and structure analysis results for **1b** and **1d**−**1f**

	1b	**1d**	**1e**	**1f**
Empirical formula	$C_{17}H_{14}OSe$	$C_{16}H_{11}ClSe$	$C_{16}H_{11}BrSe$	$C_{19}H_{16}O_2Se$
Molecular mass	313.26	317.68	362.13	355.29
Crystal system	monoclinic	triclinic	triclinic	monoclinic
Space group	$P2_1/c$ (no.14)	$P\bar{1}$ (no.2)	$P\bar{1}$ (no.2)	$P2_1/a$ (no.14)
a [Å]	7.908(2)	11.515(2)	11.215(2)	8.1968(9)
b [Å]	22.662(2)	11.202(2)	11.268(2)	13.179(2)
c [Å]	8.378(2)	5.7735(9)	5.8068(7)	14.583(2)
α [°]		92.51(1)	100.83(1)	
β [°]	113.81(1)	101.07(1)	92.93(1)	96.125(8)
γ [°]		74.01(1)	73.68(1)	
V [Å^3]	1373.7(4)	680.3(2)	691.7(2)	1566.3(3)
Z	4	2	2	4
$D_{calcd.}$ [g cm^{-3}]	1.515	1.551	1.739	1.507
$\mu_{calcd.}$ [mm^{-3}]	272.2	293.4	559.0	240.2
No. of observations	1977	2334	1998	2363
No. of variables	172	164	164	200
F_{000}	632	316	352	720
R	0.036	0.043	0.039	0.041
R_w	0.026	0.036	0.026	0.032
G.O.F.	1.73	3.26	2.65	1.73

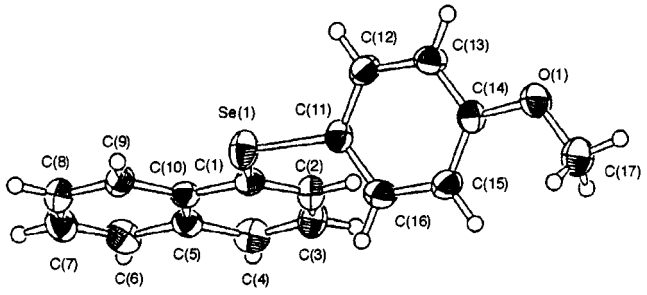

Figure 1. Structure of **1b**

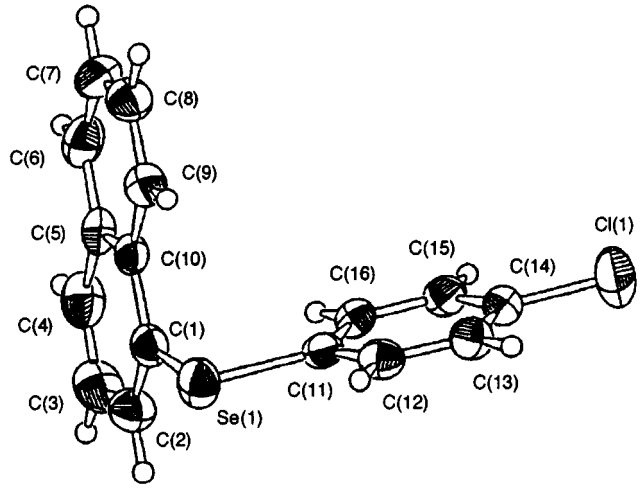

Figure 2. Structure of **1d**

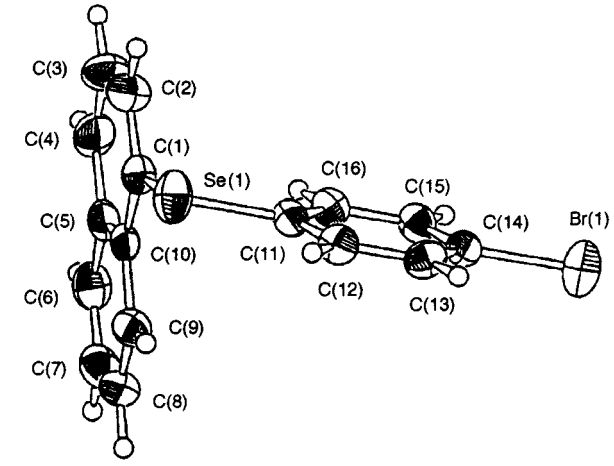

Figure 3. Structure of **1e**

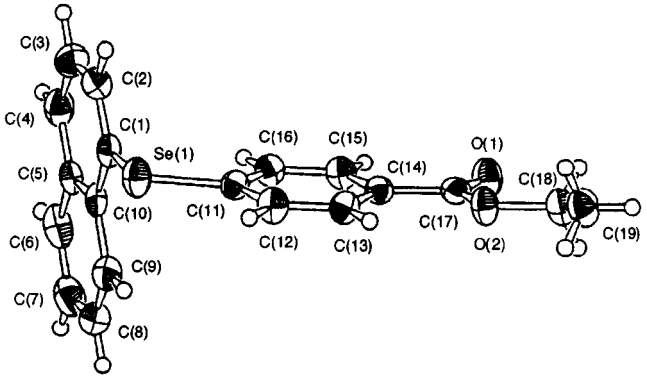

Figure 4. Structure of **1f**

gether with those of **2a**, **6a**, and **7b**. Some bond lengths (r_1 and r_2) and angles (θ_1−θ_3) are defined below. The θ_1 and θ_2 values of **1b** are larger and smaller than those of **1d**−**1f**, respectively, while the θ_3 values are almost constant among the compounds. These results show that the steric effect[17] around the Se atom is larger for type **B** than for type **A**, since the aryl group and the H atom at the 2-position are close in type **B**, but it far apart in type **A**. The trends in the angles for **6a** and **7b** lie in the same line. The type **C** structure is well established for **2a**, whose torsional angle

Table 2. Selected interatomic lengths, angles, and torsional angles of **1b** and **1d**−**1f**

	1b	**1d**	**1e**	**1f**
Interatomic lengths [Å]				
Se−C(1)	1.914(3)	1.919(4)	1.922(5)	1.920(4)
Se−C(11)	1.913(3)	1.912(3)	1.968(4)	1.913(3)
C(1)−C(2)	1.364(4)	1.364(5)	1.363(7)	1.360(5)
C(1)−C(10)	1.435(4)	1.420(4)	1.429(6)	1.415(5)
C(9)−C(10)	1.415(4)	1.409(4)	1.413(6)	1.413(5)
Angles [°]				
Se−C(1)−C(2)	123.5(3)	118.2(3)	118.4(4)	118.3(3)
Se−C(1)−C(10)	116.8(2)	121.6(3)	121.2(4)	121.1(3)
Se−C(11)−C(12)	119.2(3)	117.9(2)	118.2(3)	116.7(3)
C(1)−Se−C(11)	102.1(1)	99.3(1)	99.4(2)	101.2(1)
C(1)−C(2)−C(3)	121.5(3)	121.0(4)	121.0(5)	121.2(4)
C(1)−C(10)−C(9)	122.9(3)	123.2(3)	123.9(5)	123.7(4)
C(1)−C(10)−C(5)	118.5(3)	118.2(3)	117.6(4)	118.4(4)
Torsional angles [°]				
Se−C(1)−C(2)−C(3)	176.2(3)	−178.5(3)	178.6(4)	−175.2(3)
Se−C(1)−C(10)−C(5)	−175.4(2)	177.2(2)	−177.2(3)	175.3(2)
Se−C(1)−C(10)−C(9)	3.9(4)	−2.0(4)	2.0(6)	−5.2(5)
C(1)−Se−C(11)−C(12)	110.6(3)	174.3(3)	−174.3(4)	−179.1(3)
C(1)−Se−C(11)−C(16)	−77.6(3)	−5.9(3)	6.2(4)	3.0(3)
C(2)−C(1)−Se−C(11)	3.4(3)	100.3(3)	−100.8(4)	−99.5(3)
C(10)−C(1)−Se−C(11)	−178.9(2)	−79.3(3)	78.8(4)	85.9(3)
C(2)−C(1)−C(10)−C(5)	2.4(5)	−2.4(5)	2.4(6)	0.8(5)
C(2)−C(1)−C(10)−C(9)	−178.4(3)	178.4(3)	−178.3(4)	−179.6(3)
C(5)−C(10)−C(9)−C(8)	0.6(7)	−0.5(5)	0.3(7)	0.1(6)

of **1** were examined in discussing the conformations in solutions. The δ(2-H) and δ(8-H) values of **1** should be useful for determining the conformations as type **A** or type **B**, since they are significantly affected by the orientation of the aryl group in the compounds. Table 4 shows δ(2-H), δ(8-H), δ(C-1), δ(C-*i*), and δ(Se) values of **1** and **10**, measured in $CDCl_3$ solutions.

$$\delta\text{ (C-}i\text{) of }\mathbf{1} = 0.993 \times \delta\text{(C-}i\text{) of }\mathbf{10} + 1.408\ (r = 1.000) \quad (1)$$

$$\delta\text{(2-H) of }\mathbf{1} = 0.0236 \times \delta\text{(C-}i\text{) of }\mathbf{1} + 4.662\ (r = 0.999)\text{ for g(}\mathbf{m}\text{)} \quad (2)$$

$$\delta\text{(2-H) of }\mathbf{1} = 0.0084 \times \delta\text{(C-}i\text{) of }\mathbf{1} + 6.687\ (r = 1.000)\text{ for g(}\mathbf{n}\text{)} \quad (3)$$

$$\delta\text{(8-H) of }\mathbf{1} = 0.0053 \times \delta\text{(C-}i\text{) of }\mathbf{1} + 7.638\ (r = 1.000)\text{ for g(}\mathbf{m}\text{)} \quad (4)$$

$$\delta\text{(8-H) of }\mathbf{1} = -0.0030 \times \delta\text{(C-}i\text{) of }\mathbf{1} + 8.676\ (r = 0.896)\text{ for g(}\mathbf{n}\text{)} \quad (5)$$

Variables in the plots for the conformational determinations should be free from orientational effects, or should contain as little of such effects as possible. The δ(C-*i*) values of the *p*-YC_6H_4Se groups in **1** were ideal for these variables since an excellent correlation is observed in the plot of δ(C-*i*) of **1** versus those of **10** [Equation (1)].[18] The correlation must show that δ(C-*i*) of **1** are only slightly affected by the conformation around the Se atom in this case. Figure 5 shows the plots of δ(2-H) and δ(8-H) versus δ(C-*i*) in **1**.

Table 3. Bond lengths, angles, and torsional angles around the selenium atom in **1b** and **1d**−**1f**, together with those in **2a**, **6a**, and **7b**

	1b[a]	**1d**[a]	**1e**[a]	**1f**[a]	**2a**[b]	**6a**[b]	**7b**[c]
r[C(1)−Se] (r_1) [Å]	1.914(3)	1.919(4)	1.922(5)	1.929(4)	1.937(8)	1.909(9)	1.928(4)
r[Se−C(11)] (r_2) [Å]	1.913(3)	1.912(3)	1.908(4)	1.913(3)	1.933(8)	1.927(9)	1.918(4)
C(1)−Se−C(11) (θ_1) [°]	102.1(1)	99.3(1)	99.4(2)	101.2(1)	98.4(3)	100.6(4)	100.8(2)
C(10)−C(1)−Se (θ_2) [°]	116.8(2)	121.6(3)	121.2(4)	121.1(3)	123.1(6)	124.7(6)	120.5(3)
C(1)−C(10)−C(9) (θ_3) [°]	122.9(3)	123.2(3)	123.9(5)	123.7(4)	126.4(7)	127.5(8)	125.9(3)
Se−C(1)−C(10)−C(9) [°]	3.9(4)	−2.0(4)	2.0(6)	−5.2(5)	−8(1)	6(1)	0.9(6)
C(11)−Se−C(1)−C(10) [°]	178.9(2)	79.3(3)	78.8(4)	−85.9(3)	143.2(6)	70.0(8)	−162.8(3)
C(1)−Se−C(11)−C(12) [°]	77.6(3)	5.9(3)	6.2(4)	3.0(3)	87.7(7)	−162.0(7)	89.0(4)
Type of structure	**B**	**A**	**A**	**A**	**C**	**A**[d]	**B**

[a] G = H for the structure shown in the text. − [b] One of the structures in ref.[4e] − [c] One of the structures in ref.[4d] − [d] Type **B** for the Se−Se moiety.

C(11)−Se−C(1)−C(10) of 143.2(6)° is intermediate between those of **1b** and **1d**−**1f**.

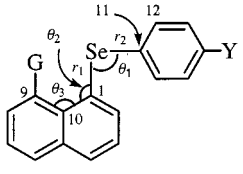

Conformations of 1a and 1c Examined by NMR

Since the structures of **1a** and **1c** could not be determined by X-ray crystallographic analysis, ^{1}H NMR chemical shifts at the 2- and 8-positions [δ(2-H) and δ(8-H), respectively] The plots were analyzed as the two correlations. The points corresponding to Y = OMe, Me, and H make up group **m** [g(**m**)], and those of Y = NO_2, COOEt, Cl, and Br belong to another group **n** [g(**n**)].[4f,16a] The correlations of δ(2-H) and δ(8-H) versus δ(C-*i*), classified by g(**m**) and g(**n**), are given in Equations (2) to (5), respectively. The excellent correlations by g(**m**) and g(**n**) support the fact that the conformations of **1a** and **1c** are closely related to that of **1b**, whose structure is type **B** in the solid state. Similar results were obtained in the plots of δ(2-H) and δ(8-H) versus δ(Se) in **1**.[19] Compound **1a** could belong to g(**n**) since the point for **1a** is very close to those for **1d** and **1e** (Figure 5). The conformation of **1a** is discussed again in the following sections.

Table 4. Some ^{1}H, ^{13}C, and ^{77}Se NMR chemical shifts of **1** and **10**

Chemical shifts[a]	Y = H (**a**)	OMe (**b**)	Me (**c**)	Cl (**d**)	Br (**e**)	COOEt (**f**)	NO_2 (**g**)
1							
δ(2-H)	7.764	7.496	7.654	7.781	7.792	7.866	7.899
δ(8-H)	8.335	8.275	8.312	8.286	8.285	8.274	8.238
δ[C-*i*(Ar)]	131.57	120.25	127.29	130.11	131.02	139.85	144.01
δ[C-1(Nap)]	126.81	131.68	130.38	128.79	128.63	127.21	125.91
δ(Se)	361.0	354.2	356.2	359.4	359.3	368.0	379.6
10							
δ[C-*i*(Ar)]	131.10	119.85	126.75	129.33	130.40	139.25	143.80
δ(C-1(Ph)]	131.10	133.05	131.93	130.52	130.44	128.78	127.11
δ(Se)	423.6	408.1	415.0	421.9	422.3	433.3	446.3

[a] Chemical shifts are relative to TMS and MeSeMe in [D]chloroform.

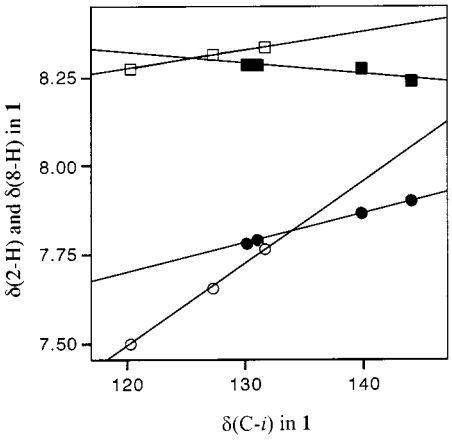

Figure 5. Plots of δ(2-H) and δ(8-H) versus δ(C-*i*) in **1**: ○, ●, □ and ■ stand for g(**m**) of δ(2-H), g(**n**) of δ(2-H), g(**m**) of δ(8-H), g(**n**) of δ(8-H), respectively

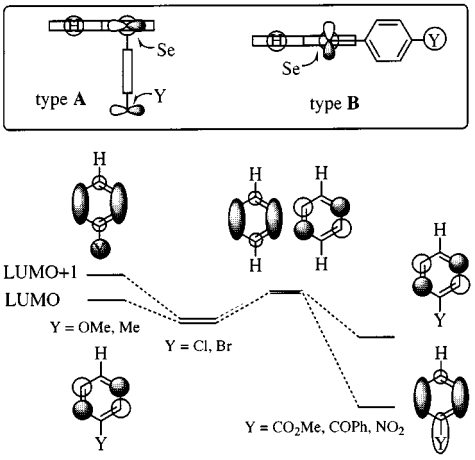

PhY / Y =	OMe	Me	H	Cl	Br	CO_2Me	COPh	NO_2	$(C_{10}H_8)$[a]
EA[b]	−1.11	−1.09	−1.15	−0.75	−0.70	−0.0[c]	0.62	1.01	(−0.2)[c]
ε(LUMO+1)[b]	−0.07	−0.37	−0.48	−0.81	−0.86	−0.70	−0.96	−1.27	(−0.65)[d]
ε(LUMO)[b]	−0.46	−0.43	−0.48	−0.86	−0.88	−1.64	−2.10	−2.92	(−1.40)[e]

[a] For naphthalenes in parenthesis. – [b] In eV. – [c] Values evaluated based on EA and ε_1. – [d] MO: – [e] MO:

Scheme 2. Perspective drawings of **1** (type **A**) and **1** (type **B**) and the correlation diagram between LUMO and LUMO+1 of benzene and substituted benzenes, together with their energies and EA, containing those of naphthalene

Factors in the Structure Determination of 1

Scheme 2 shows the perspective drawings of the type **A** and type **B** structures of **1**, together with the p-type lone pair orbitals of Se and the p-type orbitals of Y. Why are the structures of **1d**−**1f** type **A**, while that of **1b** is type **B**? Which conformation is more stable in **1a** or **1c**? The energy difference between **1a** (type **A**) and **1a** (type **B**) must contain both steric and electronic effects in the two structures of **1a**. The steric effect would not be so different for all members in **1**, if the structures are the same type. Therefore, the Y dependence in **1** must mainly be a reflection of electronic effects. We discuss the structures of **1** based on the electron affinity (EA) of C_6H_6, C_6H_5Y, and $C_{10}H_8$, the components of **1**. Their LUMO and LUMO+1 energies [ε(LUMO) and ε(LUMO+1), respectively], calculated with the B3LYP/6−311+G(d,p) method, are also employed for the discussion.

The system will be stabilized when the electrons filled in the p-type lone pair of the Se atom in **1** are effectively delocalized. The p-type lone pair of the Se atom of **1** (type **A**) is parallel to the π-orbitals of the benzene ring and the p-type orbital of Y, but it is perpendicular to those of the naphthalene ring. Therefore, the p-type lone pair of the Se atom interacts more effectively with the p-type orbital of Y through the π-orbitals of the benzene ring relative to the π-orbitals of the naphthalene ring in type **A**. On the other hand, the p-type lone pair of the Se atom interacts more strongly with the π-orbitals of the naphthalene ring in **1** (type **B**), since the two orbitals are parallel. The interaction of the p-type lone pair of the Se atom with the p-type orbital of Y through the π-orbitals of the benzene ring must be difficult in type **B** because of their orthogonality. It is natural to suppose that the structure should be type **A**, if the aryl group can delocalize the electrons at the Se atom more effectively than the naphthyl group in **1**. The structure will be type **B** if the former is less effective than the latter.

The EA of naphthalene, benzene, and the substituted benzenes can be a good measure for the electron-delocalizing ability of the corresponding groups, which are collected in Scheme 2.[20] The EA of naphthalene is estimated to be

about −0.2 eV and that of methyl benzoate is estimated to be 0.0 eV based on ε(LUMO).[21,22] The estimated EA of naphthalene is smaller than those of methyl benzoate and nitrobenzene, which is in good agreement with the type **A** structures for **1f** and **1g**. The type **B** structure for **1b** is also rationalized since the EA of anisole is much smaller than that of naphthalene. One might expect the type **B** structures for **1d** and **1e**, since the EA of the halobenzenes are smaller than that of naphthalene, which is just the opposite of what was observed. This discrepancy may come from the steric effect. The steric effect should be more severe for type **B** than for type **A**, as suggested by the observed structures. The EA of benzene and toluene are very close to that of anisole. The type **B** structure is expected for **1a** and **1c**.

We must be careful, however, in the discussion on the structures employing EA. While LUMO and LUMO+1 are degenerate in benzene, the levels separate in substituted benzenes. The two levels become more stable in chlorobenzene and bromobenzene, although they are almost degenerate. Only LUMO+1 becomes less stable in toluene and anisole. LUMO becomes much more stable than the LUMO+1 in methyl benzoate and nitrobenzene. It is worthwhile to note that the LUMO of toluene and anisole have no coefficients of atomic p-orbitals on Y nor *ipso*- and *para*-carbon atoms in PhY. This shows that the LUMO of the C_6H_4Y group in **1b** (type **A**) and **1c** (type **A**) cannot effectively interact with the filled p-type lone pair orbital of the Se atom in the compounds. LUMO+1 must work instead of LUMO. Therefore, the driving force for the formation of **1b** (type **B**) is larger than that expected based on EA, since EA is closely related to ε(LUMO) not ε(LUMO+1). Indeed, the type **B** structures are suggested for of **1a** and **1c** based on EA, but the contribution of the steric effect must also be carefully considered.

Parthasarathy et al. have suggested that there are two types of directional preferences for nonbonded atomic contacts with divalent chalcogens such as sulfur[23a] and selenium,[23b] R−Z−R′ (Z = S and Se). Type I contacts are with electrophiles that have Z···X directions in RR′Z···X where n-electrons of sulfides or selenides are located. Type II contacts are with nucleophiles tending to lie along the extension of one of sulfur's or selenium's bonds. Electrophiles and nucleophiles will interact preferentially with the HOMO of the n(Z) and with the LUMO of the σ*(Z−R) or the σ*(Z−R′), respectively. Therefore, the type **A** and type **B** structures belong to type I and type II contacts in Parthasarathy's definition, respectively, if G in 8-G-1-(RZ)$C_{10}H_6$ is assumed to be an electrophile or nucleophile (Scheme 1).[24] The type **C** structure around the chalcogen atom corresponds to the intermediate structure between type I and type II contacts.

Parthasarathy's considerations are very useful in discussing the structures of **2**−**4** and **6**−**9** where G in 8-G-1-(RZ)$C_{10}H_6$ possesses lone pair orbitals and the Z−R bond contains a relatively low-lying σ*(Se−C) bond or a low-lying σ*(Se−Se) bond. However, G in 8-G-1-(RZ)$C_{10}H_6$ is H for **1**. The H atom in a C−H bond will act neither as a good nucleophile nor as a good electrophile.[25] Therefore, the orbital interactions between the p-type lone pair orbital of the Se atom and π-orbitals of the naphthalene ring or π-orbitals of the aryl group becomes the main factor in determining the structure of **1**. In order to clarify the structural difference between **1** and **10**, molecular orbital calculations were performed on **1a**, **10a**, and the related compounds.

Results of MO Calculations

Ab initio MO calculations were performed using the Gaussian 94 and 98 programs[26,27] on **1a**, **10a**,[28] and 1-naphthaleneselenole (**11**) with the 6−311+G(d,p) basis set at the B3LYP level. The estimated conformers were further optimized with the B3LYP/6−311+G(2df,2p) method. Thermal and solvent effects were evaluated for **1a** with 6−311+G(d,p) basis set at the B3LYP level. Type **A** and type **B** notation is employed for **11** similarly to the case of **1**, when the Se−H bond is perpendicular to and in the plane of the naphthalene ring, respectively. The stable conformers and transition states were assigned based on the results of the frequency analysis.

Table 5 collects the results of the MO calculations on **1a** with the B3LYP/6−311+G(d,p) and B3LYP/6−311+G(2df,2p) methods. Almost the same energy profile was predicted for **1a** with the two methods. The results of the frequency analysis performed on **1a** with the B3LYP/6−311+G(d,p) method are also given in Table 5. Table 5 contains similar results for **11** with B3LYP/6−311+G(2df,2p) method. Table 6 summarizes the results of the calculations on **10a** with the 6−311+G(2df,2p) method, containing the data of the frequency analysis.[29] All positive frequencies were predicted for **1a** (type **A**), **1a** (type **B**), **10a** (C_2), **11** (type **A**), and **11** (type **B**), while only one imaginary frequency was predicted for each of **1a** (TS), **10a** (C_s), **10a** (C_{2v}), and **11** (TS). The motion corresponding to the imaginary frequency for **1a** (TS) was characterized mainly by the rotation around its two Se−C bonds leading to **1a** (type **A**) or **1a** (type **B**). The motion in **11** (TS) is to **11** (type **A**) or **11** (type **B**). The motion for each of **10a** (C_s) and **10a** (C_{2v}) is the rotation around the two Se−C bonds toward **10a** (C_2). Figure 6 exhibits the correlation diagrams for **1a**, **10a**, and **11**, together with the thermal corrections to Gibbs free energy at 298.15 K assuming **1a** (type **A**), **10a** (C_2), and **11** (type **A**) as the standards.

The conformer **1a** (type **A**) was evaluated to be slightly more stable than **1a** (type **B**) by 0.0005 au (1.3 kJ mol^{-1}) and **1a** (TS) as less stable than the former by 0.0011 au (2.9 kJ mol^{-1}) based on the B3LYP/6−311+G(d,p) method (Table 5). The sum of electronic and thermal free energies at 298.15 K of **1a** (type **B**) and **1a** (TS), relative to that of **1a** (type **A**), were evaluated to be 0.0005 au (1.3 kJ mol^{-1}) and 0.0032 au (8.4 kJ mol^{-1}), respectively, as shown in Table 5. The solvent effect of chloroform on the energies of **1a** was also calculated by applying the static iso-density surface-polarized continuum model (IPCM).[30] The results are shown in Table 7. The energies of **1a** (type **B**) and **1a** (TS) were evaluated to be −8.4 and 3.9 kJ mol^{-1}, respectively, relative to that of **1a** (type **A**). Consequently, the relative energies of **1a** (type **B**) and **1a** (TS) to that of **1a** (type

Table 5. Results of ab initio MO calculations for **1a** and **11** with the B3LYP/6−311+G(s,t) method

	1a (type **A**)	**1a** (type **B**)	**1a** (TS)	**1a** (type **A**)	**1a** (type **B**)	**1a** (TS)	**11** (type **A**)	**11** (type **B**)	**11** (TS)
Looking for	minimum	minimum	TS[a]	minimum	minimum	TS[a]	minimum	minimum	TS[a]
Method/G(s,t)	G(d,p)	G(d,p)	G(d,p)	G(2df,2p)	G(2df,2p)	G(2df,2p)	G(2df,2p)	G(2df,2p)	G(2df,2p)
E [au]	−3018.6355	−3018.6350	−3018.6344	−3018.6792	−3018.6789	−3018.6781	−2787.5588	−2787.5589	−2787.5576
ΔE [kJ mol^{-1}]	0.0[b]	1.3	2.9	0.0[b]	0.8	2.9	0.0[b]	−0.3	3.2
r[Se−C(1)] [Å]	1.9427	1.9481	1.9491	1.9349	1.9401	1.9406	1.9379	1.9307	1.9475
r(Se−X) [Å]	1.9433[c]	1.9391[c]	1.9411[c]	1.9348[c]	1.9319[c]	1.9327[c]	1.4731[d]	1.4685[d]	1.4717[d]
r[Se−H(8)] [Å]	2.8001	2.6615	2.7570	2.7967	2.6510	2.7522	2.8148	2.6714	2.7637
C(1)−Se−X [°]	101.19[c]	100.70[c]	100.05[c]	101.65[c]	100.93[c]	100.60[c]	96.49[d]	93.99[d]	94.99[d]
H(8)−Se−X [°]	77.35[c]	172.26[c]	123.59[c]	76.04[c]	172.59[c]	122.80[c]	62.17[d]	165.18[d]	112.46[d]
C(8)−C(9)−C(1)−Se [°]	−2.80	0.00	−3.18	−3.12	0.00	3.12	−2.10	0.00	−2.32
C(1)−C(9)−C(8)−H(8) [°]	0.77	0.00	−1.23	0.80	0.00	1.10	1.93	0.00	−0.94
C(9)−C(1)−Se−X [°]	73.32[c]	180.00[c]	125.36[c]	71.84[c]	180.00[c]	−124.22[c]	57.31[d]	180.00[d]	114.45[d]
C(1)−Se−C(*i*)−C(*o*) [°]	23.82	−91.75	−43.67	24.17	91.71	39.20			
ν_1 (character)[e] [cm^{-1}]	17.25 (?A)	11.92 (A")	−15.47 (?A)	[f]	[f]	[f]	100.10 (?A)	51.13 (A")	−157.46 (?A)
ν_2 (character)[g] [cm^{-1}]	26.64 (?A)	37.82 (A")	23.42 (?A)	[f]	[f]	[f]	160.05 (?A)	109.12 (A")	98.91 (?A)
ZPC [au][h]	0.2269	0.2270	0.2269	[f]	[f]	[f]	0.1448	0.1444	0.1442
TCF [au][i]	0.1836	0.1835	0.1857	[f]	[f]	[f]	0.1098	0.1085	0.1097
E(F) [au][j]	−3018.4518	−3018.4513	−3018.4486	[f]	[f]	[f]	−2787.4489	−2787.4504	−2787.4479
ΔE(F) [kJ mol^{-1}]	0.0[b]	1.3	8.4				0.0[b]	−3.9	2.6
Meaning	minimum	minimum	TS[a]				minimum	minimum	TS[a]

[a] Between type **A** and type **B**. − [b] Taken as the standards for the same molecule and the calculation method. − [c] X = C. − [d] X = H. − [e] Lowest frequency obtained by the frequency analysis. − [f] Not calculated. − [g] Second-lowest frequency obtained by the frequency analysis. − [h] Zero-point correction. − [i] Thermal correction to Gibbs free energy at 298.15 K. − [j] Sum of electronic and thermal Gibbs free energies at 298.15 K.

Table 6. Results of ab initio MO calculations for **10a** with the B3LYP/6−311+G(2df,2p) method

	10a (C_2)	**10a** (C_s)	**10a** (C_{2v})
Looking for	minimum	minimum	minimum
E [au]	−2864.9927	−2864.9925	−2864.9910
ΔE [kJ mol^{-1}]	0.0[a]	0.5	4.5
r[Se−C(1)] [Å]	1.9323	1.9326	1.9445
r[Se−C(1′)] [Å]	1.9323	1.9349	1.9445
C(1)−Se−C(1′) [°]	101.03	101.31	99.10
C(2)−C(1)−Se−C(1′) [°]	46.50	0.00	90.89
C(2′)−C(1′)−Se−C(1) [°]	46.50	91.42	90.89
ν_1 (character) [b] [cm^{-1}]	12.25 (B)	−21.00 (A")	−29.48 (A2)
ν_2 (character) [c] [cm^{-1}]	30.77 (A)	28.75 (A")	16.47 (B1)
ZPC [au][d]	0.1809	0.1809	0.1808
TCF [au][e]	0.1410	0.1429	0.1427
E(F) [au][f]	−2864.8518	−2864.8497	−2864.8483
ΔE(F) [kJ mol^{-1}]	0.0[a]	5.5	9.2
Meaning	minimum	saddle point	saddle point

[a] Taken as the standards. − [b] Lowest frequency obtained by the frequency analysis. − [c] Second-lowest frequency obtained by the frequency analysis. − [d] Zero-point correction. − [e] Thermal correction to Gibbs free energy at 298.15 K. − [f] Sum of electronic and thermal Gibbs free energies at 298.15 K.

A) were revised to be −8.4 and 9.4 kJ mol^{-1}, respectively, if both thermal and solvent effects were taken into account.

In the case of **11**, the type **B** conformer was evaluated to be slightly more stable than type **A** by 0.0001 au (0.3 kJ mol^{-1}) and **11** (TS) higher in energy than the former by 0.0012 au (3.2 kJ mol^{-1}) based on the B3LYP/6−311+G(2df,2p) method (Table 5). The difference in the energy profile between **1a** and **11** may come from that of the steric effect in type **B** brought by the phenyl group. The thermal effect works to stabilize **11** (type **B**) and **11** (TS) relative to **11** (type **A**): Their relative energies become −0.0015 au (−3.9 kJ mol^{-1}) and 0.0010 au (2.6 kJ mol^{-1}), respectively.

On the other hand, as shown in Table 6, the energies for **10a** (C_s) and **10a** (C_{2v}) were optimized to be higher than that of **10a** (C_2) by 0.0002 au (0.5 kJ mol^{-1}) and 0.0017 au (4.5 kJ mol^{-1}), respectively (Figure 6). The frequency analysis demonstrates that **10a** (C_2) is an energy minimum and **10a** (C_s) and **10a** (C_{2v}) must be saddle points. A fourfold transition potential without planar and perpendicular stable conformers is confirmed for **10a**, which was expected as a common characteristic for Ar−Se−R moieties. Consequently, the energy minimum of **10** is suggested to change monotonically depending on Y. The energy of **10a** (C_s) is very close to that of **10a** (C_2), which exhibits the very gentle potential curve between **10a** (C_2) and **10a** (C_s). The results must also be advantageous for the monotonical change of the structure.[16b] The relative energies of **10a** (C_s) and **10a** (C_{2v}) to that of **10a** (C_2) become 0.0021 au (5.5 kJ mol^{-1}) and 0.0035 au (9.2 kJ mol^{-1}), if the thermal effect is taken into account.

Scheme 3 shows the correlation between **1a** and **10a**. The attachments of a benzene ring to **10a** (C_s), by increasing the butadienyl skeleton, produce **1a** (type **A**) and **1a** (type **B**) as shown by (i) and (ii), respectively: The new benzene rings are drawn as dotted ones. The attachment to **10a** (C_2) yields **1a** (TS) as shown in (iii). While the attachment of the benzene ring in (i) slightly stabilizes the product relative to that in (ii),[17] a similar process (iii) destabilizes the product. These results may show that the benzene ring without the

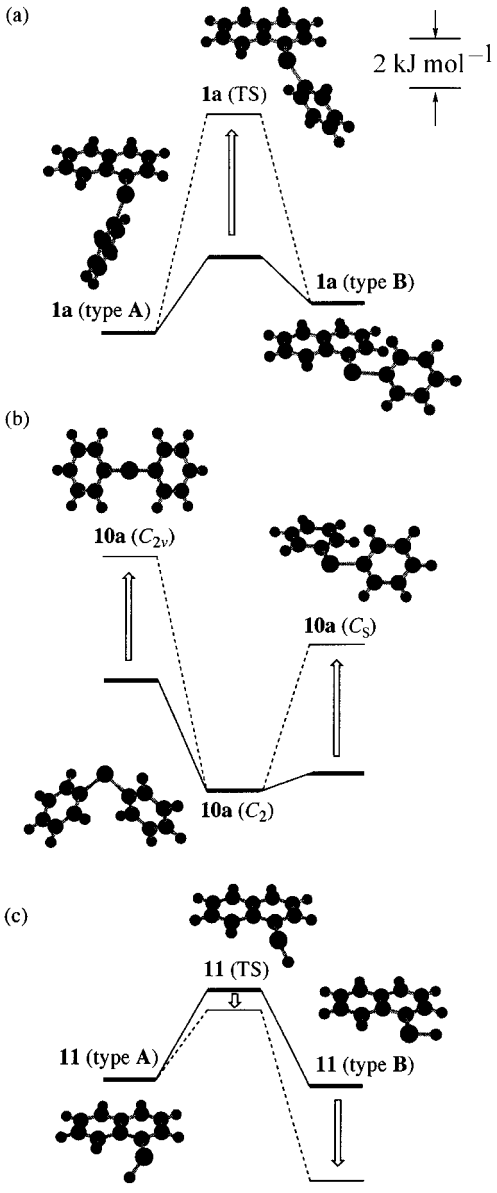

Figure 6. Energy profiles for **1a** (a), for **10a** (b), and for **11** (c); thermal corrections to Gibbs free energy at 298.15 K are also shown by arrows, where the levels are connected by dotted lines, supposing **1a** (type **A**), **10a** (C_2), and **11** (type **A**) as the standards for each

Table 7. Solvent effects on the structures of **1a**

	Full optimization[a] au (kJ mol^{-1})	Solvent effect[b] au (kJ mol^{-1})
E (type **A**)	−3018.6355 (0.0[c])	−3018.6405 (0.0[c])
E (type **B**)	−3018.6350 (1.3)	−3018.6437 (−8.4)
E (TS)	−3018.6344 (2.9)	−3018.6390 (3.9)

[a] For the energy surface. − [b] For chloroform calculated by IPCM method. − [c] Taken as the standards.

PhSe group in the naphthyl group of **1a** plays an important role in the energy profile of **1**.

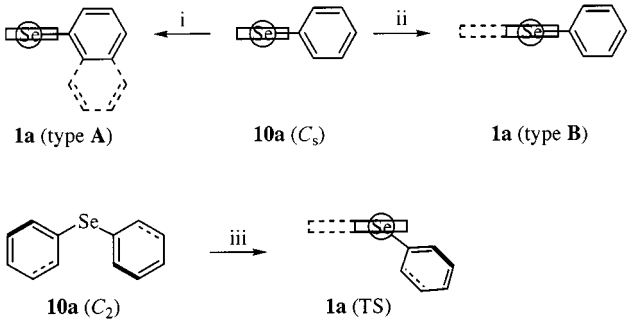

Scheme 3. Structural correlation between **1a** and **10a**

Table 8 shows the results of MO calculations performed on **1a**−**1g** with the B3LYP/6−311+G(d,p) method, although thermal and solvent effects are not considered for **1b**−**1g**. Both type **A** and type **B** structures were optimized for **1a**−**1g**, except **1f** (type **B**); **1f** (type **B**) would not be an energy minimum. The results of MO calculations suggest that type **A** is exclusive for **1g** and probably exclusive for **1f**, predominant for **1d** and **1e**, but that type **B** is more stable for **1b**. The two structures would be comparable for **1a** and **1c**. However, **1a** (type **B**) was predicted to be substantially more stable than **1a** (type **A**), if thermal and solvent effects are contained in the calculations. Table 8 collects the results of MO calculations on **10a**−**10g** with the same method. The successive change in the torsional angle on Y was predicted for the stable conformers in **10a**−**10g**.[31] These results are in accordance with the observations.[32]

The structural feature is well established for **1**. The stable structures are type **A** and type **B**, which change dramatically depending on Y in the solid state, although they must be in equilibrium in solutions in some cases.[33] On the other hand, the structure of **10** is shown to change monotonically depending on Y, as expected. This must be one of the reasons why the δ(Se) values of **1** cannot be a good measure for those of 8-G-1-(*p*-YC_6H_4Se)$C_{10}H_6$, such as **2** and **6**. Further studies on the nonbonded interactions between Se and G in 8-G-1-(*p*-YC_6H_4Se)$C_{10}H_6$ are in progress in our laboratory.

Experimental Section

General: Chemicals were used without further purification unless otherwise noted. Solvents were purified by standard methods. − Melting points are uncorrected. − ^1H, ^{13}C, and ^{77}Se NMR spectra were measured at 400, 100, and 76 MHz, respectively. The ^1H, ^{13}C, and ^{77}Se chemical shifts are given in ppm relative to those of internal $CHCl_3$, a slight contaminant in $CDCl_3$ solvent, internal $CDCl_3$ in the solvent, and external MeSeMe, respectively. − Column chromatography was performed on silica gel (Fujisilysia BW-300) and acidic alumina (E. Merck). − 1-(*p*-Anisylselanyl)naphthalene (**1b**)[4d] and phenyl (*p*-substituted phenyl) selenides (**10**)[16a] were prepared according to literature methods.

1-(Phenylselanyl)naphthalene (1a): To a solution of the sodium 1-naphthaleneselenate, prepared by the reduction of the 1,1′-dinaph-

Table 8. Calculated energies (E) for type **A** and type **B** of **1** and those of **10**, and torsional angles around the selenium atom in **10** with the B3LYP/6−311+G(d,p) method

Compound	Y = OMe	Me	H	Cl	Br	COOMe	NO_2
1							
E (type **A**) [au]	−3133.1912	−3057.9630	−3018.6355	−3478.2580	−5592.1778	−3246.5833	−3223.2005
E (type **B**) [au]	−3133.1922	−3057.9630	−3018.6350	−3478.2573	−5592.1769	[a]	−3223.1962
ΔE[b] [kJ mol^{-1}]	2.6	0.0	−1.3[c]	−1.8	−2.4	[a]	−11.3
10							
E [au]	−2979.5164	−2904.2873	−2864.9593	−3324.5818	−5438.5015	−3092.9073	−3069.5243
C(2)−C(1)−Se−C(*i*) [°]	2.67	−0.04	48.68	57.97	73.15	89.06	91.46
C(*o*)−C(*i*)−Se−C(1) [°]	89.38	91.41	48.68	40.50	24.39	1.54	0.10

[a] The type **B** structure was not optimized as a stationary point. − [b] ΔE = E (type **A**) − E (type **B**). − [c] The value was almost the same if the thermal effect was considered, but it became −8.4 if the solvent effect was calculated by the IPCM method.

thyl diselenide (990 mg, 2.40 mmol) with $NaBH_4$ (272 mg, 7.20 mmol) in aqueous THF (30 ml, 50 %, was added benzenediazonium chloride (6.00 mmol) under argon at low temperature (0−2 °C). After the usual workup, the solution was purified by chromatography on silica gel covered acidic alumina layer on the top. This gave **1a** (925 mg, 3.30 mmol, 68% yield) as a colorless oil. − ^{1}H NMR ($CDCl_3$, 400 MHz): δ = 7.18−7.21 (m, 3 H), 7.33−7.36 (m, 3 H), 7.37 (t, J = 7.8 Hz, 1 H), 7.48−7.53 (m, 2 H), 7.76 (dd, J = 1.2 and 7.1 Hz, 1 H), 7.82−7.86 (m, 2 H), 8.34 (dd, J = 2.7 and 7.1 Hz, 1 H). − ^{13}C NMR ($CDCl_3$, 100.4 MHz): δ = 125.9, 126.2, 126.7, 126.8, 127.5, 128.5, 129.1, 129.2, 129.3, 131.6, 131.6, 133.7, 134.0, 134.0. − ^{77}Se NMR ($CDCl_3$, 76.2 MHz): δ = 361.0. − $C_{16}H_{12}Se$ (283.22): calcd. C 67.85, H 4.27; found C 67.93, H 4.25.

1-(*p*-Tolylselanyl)naphthalene (1c): According to a method similar to that for **1a**, **1c** (67% yield) was obtained as a colorless oil. − ^{1}H NMR ($CDCl_3$, 400 MHz): δ = 2.29 (s, 3 H), 7.04 (d, J = 7.8 Hz, 2 H), 7.31 (d, J = 8.1 Hz, 2 H), 7.33 (t, J = 7.7 Hz, 1 H), 7.47−7.53 (m, 2 H), 7.65 (dd, J = 1.2 and 7.3 Hz, 1 H), 7.78−7.84 (m, 2 H), 8.31 (dd, J = 2.7 and 7.1 Hz, 1 H). − ^{13}C NMR ($CDCl_3$, 100.4 MHz): δ = 21.1, 126.0, 126.3, 126.8, 127.3, 127.4, 128.5, 128.6, 130.2, 130.4, 132.7, 132.7, 133.8, 134.1, 137.1. − ^{77}Se NMR ($CDCl_3$, 76.2 MHz): δ = 356.2. − $C_{17}H_{14}Se$ (297.24): calcd. C 68.69, H 4.75; found C 68.72, H 4.78.

1-(*p*-Chlorophenylselanyl)naphthalene (1d): According to a method similar to that for **1a**, **1d** (73% yield) was obtained as colorless prisms. − M.p. 54.0−55.0 °C. − ^{1}H NMR ($CDCl_3$, 400 MHz): δ = 7.15 (d, J = 8.7 Hz, 2 H), 7.24 (d, J = 8.4 Hz, 2 H), 7.39 (t, J = 7.7 Hz, 1 H), 7.49−7.54 (m, 2 H), 7.78 (dd, J = 1.1 and 7.1 Hz, 1 H), 7.83−7.88 (m, 2 H), 8.29 (dd, J = 3.3 and 6.7 Hz, 1 H). − ^{13}C NMR ($CDCl_3$, 100.4 MHz): δ = 126.0, 126.4, 127.1, 127.5, 128.6, 128.8, 129.4, 129.6, 130.1, 132.7, 132.8, 134.0, 134.2, 134.2. − ^{77}Se NMR ($CDCl_3$, 76.2 MHz): δ = 359.4. − $C_{16}H_{11}ClSe$ (317.68): calcd. C 60.49; H 3.49; found C 60.35; H 3.53.

1-(*p*-Bromophenylselanyl)naphthalene (1e): According to a method similar to that for **1a**, **1e** (69% yield) was obtained as colorless prisms. − M.p. 82.0−83.0 °C. − ^{1}H NMR ($CDCl_3$, 400 MHz): δ = 7.16 (d, J = 8.4 Hz, 2 H), 7.29 (d, J = 8.2 Hz, 2 H), 7.39 (t, J = 7.6 Hz, 1 H), 7.48−7.53 (m, 2 H), 7.79 (d, J = 7.2 Hz, 1 H), 7.83−7.89 (m, 2 H), 8.29 (dd, J = 3.4 and 6.1 Hz, 1 H). − ^{13}C NMR ($CDCl_3$, 100.4 MHz): δ = 120.8, 126.0, 126.5, 127.2, 127.6, 128.6, 128.7, 129.7, 131.0, 132.3, 132.8, 134.1, 134.2, 134.5. − ^{77}Se NMR ($CDCl_3$, 76.2 MHz): δ = 359.3. − $C_{16}H_{11}BrSe$ (362.13): calcd. C 53.07, H 3.06; found C 53.11, H 3.11.

Ethyl *p*-(1-Naphthylselanyl)benzoate (1f): According to a method similar to that for **1a**, **1f** (65% yield) wa obtained as colorless prisms. −M.p. 90.0−91.0 °C. − ^{1}H NMR ($CDCl_3$, 400 MHz): δ = 1.33 (t, J = 7.2 Hz, 3 H), 4.30 (q, J = 7.2 Hz, 2 H), 7.22 (d, J = 8.6 Hz, 2 H), 7.44 (t, J = 7.7 Hz, 1 H), 7.47−7.53 (m, 2 H), 7.79 (d, J = 8.6 Hz, 2 H), 7.87 (dd, J = 2.2 and 7.1 Hz, 1 H), 7.90−7.95 (m, 2 H), 8.27 (dd, J = 2.2 and 7.6 Hz, 1 H). − ^{13}C NMR ($CDCl_3$, 100.4 MHz): δ = 14.3, 60.9, 126.1, 126.6, 127.2, 127.4, 127.9, 128.2, 128.7, 129.4, 130.1, 130.4, 134.3, 134.5, 135.9, 139.9, 166.3. − ^{77}Se NMR ($CDCl_3$, 76.2 MHz): δ = 368.0. − $C_{19}H_{16}O_2Se$ (355.29): calcd. C 64.23, H 4.54; found C 64.19, H 4.52.

1-(*p*-Nitrophenylselanyl)naphthalene (1g): According to a method similar to that for **1a**, **1g** (75% yield) was obtained as colorless prisms. − M.p. 92.0−93.0 °C. − ^{1}H NMR ($CDCl_3$, 400 MHz): δ = 7.20 (d, J = 9.0 Hz, 2 H), 7.48 (t, J = 7.7 Hz, 1 H), 7.48−7.56 (m, 2 H), 7.90 (dd, J = 2.1 and 7.6 Hz, 1 H), 7.93 (d, J = 8.8 Hz, 2 H), 7.99 (d, J = 7.6 Hz, 2 H), 8.24 (dd, J = 1.7 and 7.6 Hz, 1 H). − ^{13}C NMR ($CDCl_3$, 100.4 MHz): δ = 123.9, 125.9, 126.2, 126.9, 127.8, 128.9, 129.0, 131.3, 134.4, 134.5, 136.8, 144.0, 146.0. − ^{77}Se NMR ($CDCl_3$, 76.2 MHz): δ = 379.6. − $C_{16}H_{11}NO_2Se$ (328.22): calcd. C 58.55, H 3.38; found C 58.62, H 3.34.

X-ray Structural Determinations: The intensity data were collected with a Rigaku AFC5R four-circle diffractometer with graphite-monochromated Mo-K_α radiation (λ = 0.71069 Å) for **1b**, **1d**, **1e**, and **1f**. Their structures were solved by heavy-atom Patterson methods, PATTY,[34] and expanded using Fourier techniques, DIRDIF94.[35] All non-hydrogen atoms were refined anisotropically. Hydrogen atoms were included but not refined. The final cycle of full-matrix least-squares refinement was based on a total of 1977 reflections for **1b**, on 2334 for **1d**, on 1998 for **1e**, and on 2363 for **1f** with 172 observed reflections [$I > 1.50\sigma(I)$] for **1b**, 164 for **1d**, 164 for **1e**, and 200 for **1f**, respectively. The refinements converged with unweighted and weighted agreement factors of $R = (\Sigma||F_o| - |F_c||)/\Sigma|F_o|$ and $R_w = \{\Sigma w(|F_o| - |F_c|)^2/\Sigma wF_o^2\}^{1/2}$. For least squares, the function minimized was $\Sigma w(|F_o| - |F_c|)^2$, where $w = (\sigma_c^2|F_o| + p^2|F_o|^2/4)^{-1}$. Crystallographic details are listed in Table 1.CCDC-162941 to -162944. Copies of the data can be obtained free of charge on applicaton to CCDC, 12 Union Road, Cambridge CB2 1EZ, UK [Fax: (internat.) + 44-1223/336-033; E-mail: deposit@ccdc.cam.ac.uk].

MO Calculations: Ab initio molecular orbital calculations were performed with an Origin computer using Gaussian 94 and 98 programs[26,27] with 6−311+G(2df,2p) and 6−311+G(d,p) basis sets at the DFT (B3LYP) level. The frequency analysis was carried out

similarly on the structures optimized with the corresponding method. Thermal (at 298.15 K) and solvent ($CHCl_3$) effects were also evaluated for **1a** by applying the static iso-density surface-polarized continuum model (IPCM)[30] with the 6−311+G(d,p) basis set at the B3LYP level.

Acknowledgments

This work was partly supported by a Grant-in-Aid for Scientific Research on Priority Areas (A) (Nos. 11120232, 11166246, and 12042259) from the Ministry of Education, Science, Sports and Culture, Japan.

[1] [1a] *Organic Sulfur Chemistry: Theoretical and Experimental Advances* (Eds.: F. Bernardi, I. G. Csizmadia, A. Mangini), Elsevier Scientific, Amsterdam, **1985**. – [1b] *The Chemistry of Organic Selenium and Tellurium Compounds* (Eds.: S. Patai, Z. Rappoport), John Wiley and Sons, New York, **1986**, vol. 1. – [1c] *The Chemistry of Organic Selenium and Tellurium Compounds* (Ed.: S. Patai), John Wiley and Sons, New York, **1986**, vol. 2. – [1d] *Organic Chemistry of Sulfur* (Ed.: S. Oae), Plenum Press, New York, **1977**. – [1e] *Organic Selenium Compounds: Their Chemistry and Biology* (Eds.: D. L. Klayman, W. H. H. Günther), Wiley, New York, **1973**. – [1f] *Organic Selenium Chemistry* (Ed.: D. Liotta), Wiley-Interscience, New York, **1987**. – [1g] M. R. Detty, M. B. O'Regan, *Tellurium-Containing Heterocycles*; Wiley, New York, **1994**. – [1h] *The Chemistry of the Ether Linkage* (Ed.: S. Patai), Wiley, New York, **1967**. – [1i] *The Chemistry of the Thiol Group* (Ed.: S. Patai), Wiley, New York, **1974**, part 1 and 2. – [1j] *The Chemistry of Ethers, Crown Ethers, Hydroxy Groups and Their Sulfur Analogues* (Ed.: S. Patai), Wiley, New York, **1980**, part 1 and 2, suppl. E. – [1k] *The Organic Chemistry of Tellurium* (Ed.: K. J. Irgolic), Gordon and Breach Science Publishers, New York, **1974**. – [1l] *Organoselenium Chemistry, A practical Approach* (Ed.: T. G. Back), Oxford University Press, Oxford, **1999**.

[2] [2a] R. S. Glass, S. W. Andruski, J. L. Broeker, *Rev. Heteroatom Chem.* **1988**, *1*, 31. – [2b] R. S. Glass, S. W. Andruski, J. L. Broeker, H. Firouzabadi, L. K. Steffen, G. S. Wilson, *J. Am. Chem. Soc.* **1989**, *111*, 4036. – [2c] R. S. Glass, L. Adamowicz, J. L. Broeker, *J. Am. Chem. Soc.* **1991**, *113*, 1065.

[3] [3a] H. Fujihara, H. Ishitani, Y. Takaguchi, N. Furukawa, *Chem. Lett.* **1995**, 571. – [3b] H. Fujihara, M. Yabe, J.-J. Chiu, N. Furukawa, *Tetrahedron Lett.* **1991**, *32*, 4345. – [3c] N. Furukawa, T. Fujii, T. Kimura, H. Fujihara, *Chem. Lett.* **1994**, 1007. – [3d] H. Fujihara, R. Saito, M. Yabe, N. Furukawa, *Chem. Lett.* **1992**, 1437.

[4] [4a] W. Nakanishi, *Chem. Lett.* **1993**, 2121. – [4b] W. Nakanishi, S. Hayashi, S. Toyota, *Chem. Commun.* **1996**, 371. – [4c] W. Nakanishi, S. Hayashi, H. Yamaguchi, *Chem. Lett.* **1996**, 947. – [4d] W. Nakanishi, S. Hayashi, A. Sakaue, G. Ono, Y. Kawada, *J. Am. Chem. Soc.* **1998**, *120*, 3635. – [4e] W. Nakanishi, S. Hayashi, S. Toyota, *J. Org. Chem.* **1998**, *63*, 8790. – [4f] S. Hayashi, W. Nakanishi, *J. Org. Chem.* **1999**, *64*, 6688. – [4g] W. Nakanishi, S. Hayashi, T. Uehara, *J. Phys. Chem. A* **1999**, *103*, 9906.

[5] [5a] M. Iwaoka, S. Tomoda, *J. Am. Chem. Soc.* **1994**, *116*, 4463. – [5b] M. Iwaoka, S. Tomoda, *J. Am. Chem. Soc.* **1996**, *118*, 8077. – [5c] M. Iwaoka, H. Komatsu, S. Tomoda, *Chem. Lett.* **1998**, 581. – [5d] H. Komatsu, M. Iwaoka, S. Tomoda, *Chem. Commun.* **1999**, 205.

[6] [6a] K.-D. Asmus, *Acc. Chem. Res.* **1979**, *12*, 436. – [6b] W. K. Musker, *Acc. Chem. Res.* **1980**, *13*, 200. – [6c] H. Fujihara, N. Furukawa, *J. Mol. Struct. (Theochem)* **1989**, *186*, 261.

[7] [7a] F. B. Mallory, *J. Am. Chem. Soc.* **1973**, *95*, 7747. – [7b] F. B. Mallory, C. W. Mallory, M.-C. Fedarko, *J. Am. Chem. Soc.* **1974**, *96*, 3536. – [7c] F. B. Mallory, C. W. Mallory, W. M. Ricker, *J. Am. Chem. Soc.* **1975**, *97*, 4770. – [7d] F. B. Mallory, C. W. Mallory, W. M. Ricker, *J. Org. Chem.* **1985**, *50*, 457. – [7e] F. B. Mallory, C. W. Mallory, M. B. Baker, *J. Am. Chem. Soc.* **1990**, *112*, 2577. – [7f] L. Ernst, K. Ibrom, *Angew. Chem. Int. Ed. Engl.* **1995**, *34*, 1881. – [7g] L. Ernst, K. Ibrom, K. Marat, R. H. Mitchell, G. J. Bodwell, G. W. Bushnell, *Chem. Ber.* **1994**, *127*, 1119.

[8] [8a] F. B. Mallory, E. D. Luzik, Jr., C. W. Mallory, P. J. Carroll, *J. Org. Chem.* **1992**, *57*, 366. – [8b] F. B. Mallory, C. W. Mallory, *J. Am. Chem. Soc.* **1985**, *107*, 4816.

[9] [9a] I. Johannsen, H. Eggert, *J. Am. Chem. Soc.* **1984**, *106*, 1240. – [9b] I. Johannsen, H. Eggert, S. Gronowitz, A.-B. Hörnfeldt, *Chem. Scr.* **1987**, *27*, 359. – [9c] H. Fujihara, H. Mima, T. Erata, N. Furukawa, *J. Am. Chem. Soc.* **1992**, *114*, 3117.

[10] [10a] G. Gafner, F. H. Herbstein, *Acta. Cryst.* **1962**, *15*, 1081. – [10b] M. A. Davydova, Yu. T. Struchkow, *Zh. Strukt. Kim.* **1962**, *3*, 184. – [10c] M. A. Davydova, Yu. T. Struchkow, *Zh. Strukt. Kim.* **1968**, *9*, 1968. – [10d] H. Bock, M. Sievert, Z. Havlas, *Chem. Eur. J.* **1998**, *4*, 677. – [10e] R. D. Jackson, S. James, A. G. Orpen, P. G. Pringle, *J. Organomet. Chem.* **1993**, *458*, C3.

[11] For X-ray crystallographic study of 1-(oxy)naphthalene: – [11a] W. B. Schweizer, G. Procter, M. Kaftory, D. Dunitz, *Helv. Chim. Acta.* **1978**, *61*, 2783. – [11b] G. Procter, D. Britton, D. Dunitz, *Helv. Chim. Acta.* **1981**, *64*, 471.

[12] W. R. Blackmore, S. C. Abrahams, *Acta Crystallogr.* **1955**, *8*, 323.

[13] W. Nakanishi, S. Hayashi, unpublished results.[14]

[14] The type **B** structure is established for all members of **8** and **9**. We called the change in the structures of **1d**−**1g** from type **A** to type **B** in **8d**−**8g** and **9d**−**9g** as G dependence. In such cases, the plot of δ(Se) of **9** versus those of **8** gave an excellent correlation [Equation (a)]. However, the plot of δ(Se) of **1** versus those of **8** must be analyzed as two correlations [Equations (b) and (c)], which strongly suggests that the structure for g(**m**) is different from that for g(**n**) in **1**.

δ(Se) of **9** = 0.898 × δ(Se) of **8** + 40.14 $r = 0.999$ ($n = 7$) (a)

δ(Se) of **1** = 0.463 × δ(Se) of **8** + 147.95 $r = 0.994$ for g(**m**) (b)

δ(Se) of **1** = 0.941 × δ(Se) of **8** − 68.02 $r = 0.999$ for g(**n**) (c)

[15] [15a] See footnote 17 of ref.[4f] – [15b] Although the plot of δ(Se) of **2** versus those of **1** gives a rather poor correlation, as shown in Equation (d), the correlation becomes excellent if the points corresponding to Y = OMe and Me are omitted [Equation (e)]. – [15c] See footnote 16 of ref.[4f]

δ(Se) of **1** = 0.686 × δ(Se) of **2** + 71.6 $r = 0.979$ ($n = 7$) (d)

δ(Se) of **1** = 0.825 × δ(Se) of **2** + 11.1 $r = 0.999$ ($n = 5$) (e)

[16] [16a] W. Nakanishi, S. Hayashi, *J. Phys. Chem. A* **1999**, *103*, 6074. – [16b] See also: G. Montaudo, P. Finocchirdo, S. Caccamese, *J. Org. Chem.* **1973**, *38*, 170.

[17] [17a] The effect is accelerated by the buttressing effect of the phenyl ring without the Se atom in the naphthalene ring if **1** is compared with **10**. – [17b] For the buttressing effect, see: M. Aoki, M. Nakamura, M. Oki, *Bull. Chem. Soc. Jpn.* **1982**, *55*, 2512. – [17c] G. Yamamoto, M. Suzuki, M. Oki, *Bull. Chem. Soc. Jpn.* **1983**, *56*, 809. – [17d] R. N. Armstrong, H. L. Ammon, J. N. Darnow, *J. Am. Chem. Soc.* **1987**, *109*, 2077. – [17e] M. Decouzon, P. Ertl, O. Exner, J. F. Gal, P. C. Maria, *J. Am. Chem. Soc.* **1993**, *115*, 12071. – [17f] C. D. Braddock, S. C. Tucker, J. M. Brown, *Bull. Chem. Chim. Fr.* **1997**, *134*, 399.

[18] A good correlation is also obtained in the plot of δ(C-*i*) of **1** versus δ(C-*p*) of C_6H_5Y,[36] which supports the expectation on δ(C-*i*) of **1**.

δ(C-*i*) of **1** = 1.67 × δ(C-*p*) of C_6H_5Y − 82.3 $r = 0.995$ (f)

[19] The correlations for the plots of δ(2-H) and δ(8-H) versus δ(Se) in **1** classified by g(**m**) and g(**n**) are as follows.

δ(2-H) of **1** = 0.0364 × δ(Se) of **1**−5.357 $r = 0.944$ for g(**m**) (g)

δ(2-H) of **1** = 0.0057 × δ(Se) of **1** + 5.739 $r = 0.958$ for g(**n**) (h)

δ(8-H) of **1** = 0.0081 × δ(Se) of **1** + 5.420 $r = 0.933$ for g(**m**) (i)

δ(8-H) of **1** = −0.0023 × δ(Se) of **1** + 9.114 r = 0.981 for g(**n**) (j)

[20] [20a] S. G. Lias, J. E. Bartmess, J. L. Holmes, R. D. Levin, J. F. Liebman, W. G. Mallard, ("Gas-Phase Ion and Newtral Thermochemistry"), *J. Phys. Chem. Ref. Data*, **1988**, *1* 17, suppl. − [20b] K. D. Jordan, P. D. Burrow, *Acc. Chem. Res.* **1978**, *11*, 341. − [20c] K. D. Jordan, P. D. Burrow, *Chem. Res.* **1987**, *87*, 557.

[21] A good correlation between the EA and ε(LUMO) at the DFT level is suggested: *Chemical Hardness* (Ed.: R. G. Pearson), Wiley-VCH, New York, **1997**, p. 38.

[22] The EA of PhY correlates very well with its ε(LUMO), calculated by the B3LYP/6−311+G(d,p) method [EA = −0.900 × ε(LUMO) − 1.484 (r = 0.993)]. The EA of methyl benzoate and naphthalene are estimated by applying the correlation (−0.008 and −0.224 eV, respectively). The EA of anthracene is 0.60 eV[20] and its ε(LUMO) and ε(LUMO+1) are evaluated to be −0.75 and −2.02 eV, respectively, by the same method. If the data of anthracene are added to the plot, the EA of naphthalene is estimated to be −0.185 eV. The estimated value becomes −0.065 eV if only the data of benzene, naphthalene, and anthracene are used.

[23] [23a] R. E. Rosenfield, Jr., R. Parthasarathy, J. D. Dunitz, *J. Am. Chem. Soc.* **1977**, *99*, 4860. − [23b] N. Ramasubbu, R. Parthasarathy, *Phosphorus Sulfur* **1987**, *31*, 221.

[24] The type **A**−type **B** pairing is equal to the type I−type II pairing, which is stabilized through the electron donor−acceptor interaction. The type **C** structure around the two chalcogen atoms must be equal to the type III pairing, of which θ values at both sites should be almost the same.

[25] The first ionization potentials for ethane and ethene are reported to be 11.52 and 10.507 eV, respectively.[20] Although the electron affinity of ethene is −1.74 eV,[20] that of ethane would be substantially smaller than this value. The results show that the ability of a C−H bond as a donor and an acceptor must be very small.

[26] M. J. Frisch, G. W. Trucks, H. B. Schlegel, P. M. W. Gill, B. G. Johnson, M. A. Robb, J. R. Cheeseman, T. Keith, G. A. Petersson, J. A. Montgomery, K. Raghavachari, M. A. Al-Laham, V. G. Zakrzewski, J. V. Ortiz, J. B. Foresman, J. Cioslowski, B. B. Stefanov, A. Nanayakkara, M. Challacombe, C. Y. Peng, P. Y. Ayala, W. Chen, M. W. Wong, J. L. Andres, E. S. Replogle, R. Gomperts, R. L. Martin, D. J. Fox, J. S. Binkley, D. J. Defrees, J. Baker, J. P. Stewart, M. Head-Gordon, C. Gonzalez, J. A. Pople, *Gaussian 94*, *Revision D.4*, Gaussian Inc., Pittsburgh PA, **1995**.

[27] M. J. Frisch, G. W. Trucks, H. B. Schlegel, G. E. Scuseria, M. A. Robb, J. R. Cheeseman, V. G. Zakrzewski, J. A. Montgomery, Jr., R. E. Stratmann, J. C. Burant, S. Dapprich, J. M. Millam, A. D. Daniels, K. N. Kudin, M. C. Strain, O. Farkas, J. Tomasi, V. Barone, M. Cossi, R. Cammi, B. Mennucci, C. Pomelli, C. Adamo, S. Clifford, J. Ochterski, G. A. Petersson, P. Y. Ayala, Q. Cui, K. Morokuma, D. K. Malick, A. D. Rabuck, K. Raghavachari, J. B. Foresman, J. Cioslowski, J. V. Ortiz, A. G. Baboul, B. B. Stefanov, G. Liu, A. Liashenko, P. Piskorz, I. Komaromi, R. Gomperts, R. L. Martin, D. J. Fox, T. Keith, M. A. Al-Laham, C. Y. Peng, A. Nanayakkara, M. Challacombe, P. M. W. Gill, B. Johnson, W. Chen, M. W. Wong, J. L. Andres, C. Gonzalez, M. Head-Gordon, E. S. Replogle, and J. A. Pople, *Gaussian 98*, *Revision A.9*, Gaussian, Inc., Pittsburgh PA, **1998**.

[28] The energy profile of benzeneselenol (ref.[16a]) calculated with the B3LYP/6−311+G(d,p) method is close to that of **10a**, although there is no C_2 symmetry in the selenol.

[29] The frequency analysis for **10a** with the B3LYP/6−311+G(d,p) method gave slightly different results. One imaginary (negative) frequency was predicted for each of **10a** (C_2), **10a** (C_{2v}), and **10a** (C_s). All positive frequencies were predicted for two **10a** (C_1), which are very close to **10a** (C_2) in geometry. This fact may show that the energy surface near **10a** (C_2) is very flat as pointed out for the corresponding structure of PhSeH (**11**). The energy difference between **10a** (C_s) and **10a** (C_1) is less than 3×10^{-5} au (0.08 kJ mol^{-1}).

[30] J. B. Foresman, T. A. Keith, K. B. Wiberg, J. Snoonian, M. J. Frisch, *J. Phys. Chem.* **1996**, *100*, 16098.

[31] The structure of *p*-MeOCOC$_6$H$_4$SePh (**10f**) was determined by the X-ray crystallographic analysis. The torsional angles of C(2)−C(1)−Se−C(*i*) and C(*o*)−C(*i*)−Se−C(1) are 108(1) and 12(1)°, respectively (R = 0.076), while the calculated values are 1.5 and 89.1°, respectively (Table 7). The observed torsional angles are close to the calculated values. However, the observed structure of **10f** is closer to that of the C_2 symmetry than the calculated one. W. Nakanishi, S. Hayashi, unpublished results.

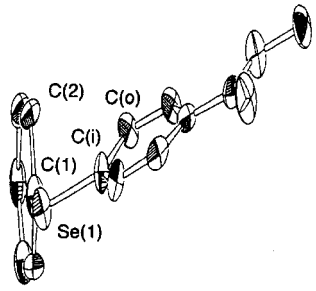

[32] Since the energy difference between **10a** (C_2) and **10a** (C_s) is very small, the average (or substantial) torsional angles of **10b**−**10g** may be closer to that of **10a** (C_2) in solutions than those predicted by the MO calculations given in Table 8.

[33] We should comment on the type **B** structure of **7b**. One might realize that the type **B** structure of **7b** needs no assistance of F at the 8-position, since the structure of **1b** is also demonstrated to be type **B**. Details will be reported in a forthcoming paper.

[34] P. T. Beurskens, G. Admiraal, G. Beurskens, W. P. Bosman, S. Garcia-Granda, R. O. Gould, J. M. M. Smits, C. Smykalla, *The DIRDIF program system*, Technical Report of the Crystallography Laboratory, University of Nijmegen, The Netherlands, **1992**.

[35] P. T. Beurskens, G. Admiraal, G. Beurskens, W. P. Bosman, R. de Gelder, R. Israel, J. M. M. Smits, *The DIRDIF-94 program system*, Technical Report of the Crystallography Laboratory, University of Nijmegen, The Netherlands, **1994**.

[36] ^{13}*C NMR Spectroscopy: Methods and Applications in Organic Chemistry* (Eds.: E. Breitmare, W. Voelter), 2nd ed., Verlag Chemie, Weinheim, **1978**.

Received February 21, 2001
[O01090]